International Journal of Pharmaceutics 573 (2020) 118736

Contents lists available at ScienceDirect

International Journal of Pharmaceutics

journal homepage: www.elsevier.com/locate/ijpharm

Amplification of tumor antigen presentation by NLGplatin to improve chemoimmunotherapy

Yong Zhu[a,1], Lei Xing[a,b,c,d,1], Xiao Zheng[e,1], Chen-Xi Yang[a], Yu-Jing He[a], Tian-Jiao Zhou[a], Qing-Ri Jin[f,*], Hu-Lin Jiang[a,b,c,d,*]

[a] State Key Laboratory of Natural Medicines, Department of Pharmaceutics, China Pharmaceutical University, Nanjing 210009, China
[b] Jiangsu Key Laboratory of Druggability of Biopharmaceuticals, China Pharmaceutical University, Nanjing 210009, China
[c] Jiangsu Key Laboratory of Drug Screening, China Pharmaceutical University, Nanjing 210009, China
[d] Jiangsu Key Laboratory of Drug Discovery for Metabolic Diseases, China Pharmaceutical University, Nanjing 210009, China
[e] State Key Laboratory of Natural Medicines, Key Laboratory of Drug Metabolism and Pharmacokinetics, China Pharmaceutical University, Nanjing 210009, China
[f] Key Laboratory of Applied Technology on Green-Eco-Healthy Animal Husbandry of Zhejiang Province, College of Animal Science and Technology, Zhejiang A&F University, Lin'an, Zhejiang 311300, China

ARTICLE INFO

Keywords:
NLGplatin
Calreticulin
IDO inhibitor
Immunotherapy
Oxaliplatin

ABSTRACT

Oxaliplatin is a chemotherapeutic agent widely used in cancer treatment whereas its immunosuppressive effect hinders the progress of immunotherapy. Here we have synthesized a new compound NLGplatin constructed by combining oxaliplatin (OXA) and indoleamine 2,3-dioxygenase (IDO) inhibitor NLG919. The NLGplatin acquires chemotherapeutic properties of OXA and can activate the immune system, and also retains the ability to inhibit IDO enzyme activity without affecting the proliferation of immune cells. This difunctional drug has a great potential to achieve effective cancer chemoimmunotherapy.

1. Introduction

At present, chemotherapy is still one of the main means in various types of cancers treatment (Vanneman and Dranoff, 2012). However, continuous chemotherapy can cause enormous damage to immune system, especially platinum drugs elicit obvious myelosuppression (Uyttenhove et al., 2003). Oxaliplatin (OXA), as a first-line platinum-based chemotherapeutic drug, performs strongly inhibition on proliferation of white blood cells and further causing immunosuppression (Galluzzi et al., 2012). Recently, how to avoid immunosuppression caused by platinum-based drug becomes a hotspot. On the other hand, the overexpressed indoleamine 2,3-dioxygenase (IDO) enzyme in various tumors, which is an important negative feedback protein that can degrade tryptophan (L-Trp) in tumors involved in forming an immunosuppressive environment through the IFN-γ pathway, can further aggravate immunosuppression [Lob et al., 2009; Chen et al., 2016; Muller and Prendergast, 2005]. To address this issue, one of hotspots in the recent tumor immunotherapy is focused on IDO inhibitors. Specifically, IDO inhibitor and chemotherapeutic drug are encapsulated into silicon nanoparticles or coupled to nanomaterials to prepare nanoformulation (Chen et al., 2016; Lu et al., 2017). Also, some Pt prodrugs were rationally designed to achieve better anti-tumor effect (Wang et al., 2018; Liang et al., 2018). Nevertheless, the nano drug delivery system maintains the advantages of two drugs but they have the problems like unstable release, complex and difficult preparation procedure (Chen et al., 2017; Xing et al., 2018; Qiao et al., 2018; Zeng et al., 2018; Fan et al., 2019). In comparison with nanoformulation, small molecule drug wildly used in cancer treatment, especially difunctional drug including chemotherapy and immunotherapy, shows a promising solution to overcome the weakness in nano drug delivery system (Gabano et al., 2014; Shi et al., 2017).

In this work, we intend to design a new drug containing two features of chemotherapy and immunotherapy (Lake and Robinson, 2005). As shown in Scheme 1, such drug, NLGplatin, was synthesized by coordination reaction of OXA and NLG919. It is very easy to be obtained and retains the features of OXA which is able to kill tumor cells and promote exposure of calreticulin (CRT) and NLG919 (a highly IDO-selective inhibitor with an EC_{50} of 75 nM) used for solving the immunosuppression of chemotherapy (Obeid et al., 2007; Chen et al., 2016; Li et al., 2014; Green et al., 2009). There is no complicated

* Corresponding authors at: State Key Laboratory of Natural Medicines, Department of Pharmaceutics, China Pharmaceutical University, Nanjing 210009, China (H.-L. Jiang).
E-mail addresses: jin@zafu.edu.cn (Q.-R. Jin), jianghulin3@gmail.com (H.-L. Jiang).
[1] These authors contributed equally to this work.

https://doi.org/10.1016/j.ijpharm.2019.118736
Received 15 July 2019; Received in revised form 14 September 2019; Accepted 24 September 2019
Available online 19 November 2019
0378-5173/

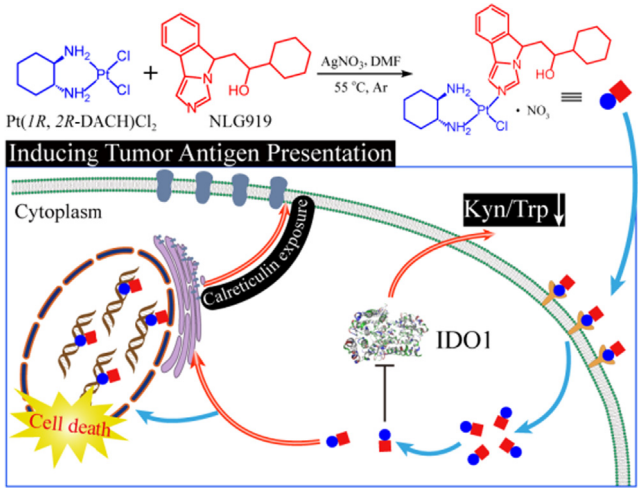

Scheme 1. Synthesis and intracellular mechanism of NLGplatin.

delivery system or endless procedure in preparation but truly maintaining the features of two drugs.

2. Materials and methods

2.1. Materials

Pt(*1R, 2R*-DACH)Cl_2 (purity > 95%) and oxaliplatin (OXA, > 98%) were purchased from Shandong Boyuan Pharmaceutical Co., Ltd. (China). NLG919 (purity > 98%) and 1-methy-dl-tryptophan (1-MT, purity > 98%) was obtained from Shanghai Ruiyan Biological Ltd. (China). Silver nitrate ($AgNO_3$, > 99%) and L-kynurenine (L-Kyn, > 98%) were purchased from Sigma Aldrich (China). Chloroform (TCM), acetone (DMK), acetic acid (HAc), ether absolute (DEE), methanol (MeOH) were all purchased from Nanjing Chemical Reagent Co., Ltd. (China, analytical purity). KCl Electrolytic Conductivity Solution (GBW (E) 130108) was obtained from National Institute of Metrology (China). N′, N-Dimethylformamide (DMF, China, super dry, > 99.8%) and dimethyl sulfoxide-d_6 (DMSO-d_6, > 99.8%) were purchased form J &K Scientific Ltd. (China). Acetonitrile was obtained from TeleChem International Inc. (USA, HPLC, > 99%). Dulbecco's Modified Eagle's Medium (DMEM), Roswell Park Memorial Institute 1640 Medium (RPMI 1640), Hanks' Balanced Salt Solution (HBSS) and fetal bovine serum (FBS) were obtained from Jiangsu Keygen Biotech Corp., Ltd. Reactive Oxygen Species Assay Kit (S0033) and Genomic DNA Mini Preparation Kit with Spin Column (D0063) were obtained from Beyotime Biotechnology. Anti-Calreticulin antibody (ab2907 and ab92516) and Goat Anti-Rabbit IgG Alexa Fluor® 488 antibody (ab150077) were all purchased from Abcam (UK). Mouse CD 8α PE, mouse CD 4 APC, mouse CD16/32 and CFSE were obtained from BD Pharmingen (USA). Anti-mouse CD3ε antibody was purchased from Thermo Fisher Scientific (USA). Mouse IL-2 protein was obtained from Bio-Techne China Co., Ltd. (China). Human IFN-γ was purchased from Sion Biological Inc. (USA). All of the chemicals were used as supplied without further purification.

2.2. Animals

Female BALB/c mice (6–8 weeks) were purchased from Shanghai Sippr-BK laboratory animal Co. Ltd. All animal care and procedures were in line with the guidelines approved by the Institutional Animal Ethical Committee of China Pharmaceutical University.

2.3. Cell culture

4T1 murine breast cancer cells and HeLa human cervical cancer cells were maintained in Dulbecco's Modified Eagle's Medium (DMEM) supplemented with 10% fetal bovine serum (FBS) and 1% penicillin-streptomycin at 37 °C in a humidified environment with 5% CO_2. Splenocytes were maintained in Roswell Park Memorial Institute 1640 Medium (RPMI 1640) supplemented with 10% fetal bovine serum (FBS) and 1% penicillin-streptomycin at 37 °C in a humidified environment with 5% CO_2. All cell lines used in this work were obtained from ATCC (Manassas, VA).

2.4. Synthesis of NLGplatin

NLGplatin was synthesized by one-pot synthesis: 200 mg (0.53 mmol) Pt(*1R, 2R*-DACH)Cl_2 was mixed with 88.47 mg (0.52 mmol) of silver nitrate and 151.53 mg (0.54 mmol) of NLG919 in DMF solution in the protection of argon at 55 °C to react about 24 h. Purified NLGplatin was obtained by column chromatography: first, reaction solution was centrifuged at 2500 rpm about 5 min after being cooled down to room temperature in order to collect supernatant. Second, column chromatography was used to separate product from mixture by developing solvent which was TCM:MeOH:DMK:HAc = 10:0.5:4:0.1. Then, crude product which was dissolved in DMF solution was dropped into DEE solution before being centrifuged at 2000 rpm about 1 min to gather precipitation. Finally, the precipitation was washed by DEE solution twice and put into vacuum drying at 40 °C for 24 h. The yield was 145.55 mg (~44.11%).

2.5. Conductivity measurement of NLGplatin

Conductance curve of NLGplatin was determined by conductivity measurement. KCl electrolytic conductivity solution was used to calibrate conductivity meter at 25 ± 0.5 °C. A series of different concentration with Pt(*1R, 2R*-DACH)Cl_2, NLG919 and NLGplatin were prepared by ultrasound for 30 min after dissolving in ultra-pure water. All the samples were tested by conductivity meter at 25 ± 0.5 °C in constant temperature water bath.

2.6. Identification of nitrate ion by RP-HPLC

Identification of nitrate ion was studied by RP-HPLC. Pt(*1R, 2R*-DACH)Cl_2, NLG919, NLGplatin and $NaNO_3$ were dissolving in 25 mL mobile phase after precision weighing about 2.5 mg. A 20 μL of each solution was injected using SHIMADZU Shim-pack C18 column and 70:30 water (containing 4.2% v/v phosphoric acid): acetonitrile buffer of pH 3.0 as mobile phase. The wavelength used for experiments were 215 nm and 270 nm and the flow rate was 0.5 mL/min.

2.7. Cellular uptake of oxaliplatin and NLGplatin

4T1 cells were seeded at a density of 3×10^5 cells/mL on each well of a six well plate and allowed to grow overnight. Oxaliplatin and NLGplatin treated 4T1 cancer cells at concentration of 20 μM for 1 h. After treatment, cells washed with hanks for twice and trypsinized, repeatedly washed, and centrifuged at 1500 revolutions per min (rpm) for 5 min. Nuclear uptake of oxaliplatin and NLGplatin were followed by Genomic DNA Mini Preparation Kit with Spin Column. Cellular uptake and nuclear uptake of oxaliplatin and NLGplatin in whole cells were all determined by inductively coupled plasma mass spectrometry (ICP-MS).

2.8. Apoptosis of NLGplatin by Annexin V assay

In order to detect the apoptosis of NLGplatin, 4T1 cells were seeded at a density of 3×10^5 cells/mL on each well of a six well plate.

Medium was changed and the cells were treated with 100 μM oxaliplatin, 100 μM NLGplatin and mixture of oxaliplatin and NLG919 (both are 100 μM) for different times at 37 °C. The cells were trypsinized, repeatedly washed, and centrifuged at 1500 rpm for 5 min, and the supernatants were discarded. Cells density was determined and cells were resuspended in 500 μL binding buffer. To 200 μL of cell suspension, 5 μL annexin V-FITC and 5 μL propidium iodide (PI) working solution were added, incubated for 15 min at room temperature. After the incubation period, samples were gently vortex keeping the samples on ice and the samples were analyzed on flow cytometer immediately.

2.9. Intracellular ROS generation assay

To determine the intracellular ROS level, 4T1 cells were seeded at a density of 3×10^5 cells/mL one day before adding drugs. After growing overnight, medium was changed and the cells were treated with different drugs for 8 h at 37 °C. Then, drugs were removed and DCFH-DA (1:1000) were added into six well plate incubated for 20 min. After that, cells were trypsinized, collected to wash, and centrifuged at 1500 rpm for 5 min, the supernatants were discarded at last. Cells were resuspended in 300 μL hanks solution. Samples were analyzed on flow cytometer immediately.

2.10. CRT expression in 4T1 cells

For surface detection of CRT, cells were washed twice with hanks and fixed in 1% paraformaldehyde in hanks for 15 min. Cells were then washed twice in hanks, and 5% goat serum was used to block for 30 min before rabbit anti-mouse CRT primary antibody, diluted in FACS buffer (1× hanks, 5% fetus bovine serum, and 0.1% sodium azide) adding in at 4 °C overnight. After incubation period, cells were washed three times before Alexa 488-conjugated secondary antibody diluted in FACS buffer. Nuclear were staining with Hoechst 33,342 dye (1/200) in hanks for 15 min at 37 °C before visualizing under LSM 700 confocal microscope. High magnification images were obtained under 63× objective lens. In some experiments, cells were incubated with 5 μL propidium iodide before assessment in flow cytometer. The data were expressed as fold-increase in mean fluorescence intensity (MFI) compared to the untreated control.

2.11. Cell-based IDO assays

The IDO inhibitory effect of NLGplatin was tested by an *in vitro* IDO assay. HeLa cells were seeded in a 96-well plate at density of 1×10^4 cells/well and allowed to grow overnight. Recombinant human IFN-γ was then added to each well with a final concentration of 50 ng/mL. At the same time, various concentrations of NLG919, NLGplatin, mixture of oxaliplatin and NLG919 or 1-MT (concentrations: 0.11–20 μM) were added to the cells. After 48 h of incubation, 150 μL of the supernatants per well was transferred to a new 96-well plate. Seventy-five microliter of 30% trichloroacetic acid was added into each well and the mixture was incubated at 50 °C for 30 min to hydrolyse N-formylkynurenine to kynurenine. Next, Supernatants were transferred to a new 96-well plate and mixed with equal volume of Ehrlich reagent (2% p-dimethylaminobenzaldehyde w/v in glacial acetic acid), and incubated for 15 min at room temperature. Reaction product was measured at 490 nm by Multiskan GO microplate reader.

2.12. T-cell proliferation study

Splenocyte suspensions were generated from BALB/c mice by passage through the nylon wool columns after lysing of red blood cells. Splenocytes (2×10^6 cells per well, pre-stained with 5-(and 6)-carboxyfluorescein diacetate (CFSE)) were seeded in a U-type 96-well plate. Various concentrations of NLG919, NLGplatin or mixture of oxaliplatin and NLG919 were added to the cells. To measure the T lymphocyte proliferation, 5 μg/mL anti-CD3ε was coated into the bottom of the plate before coculture. And 10 ng/mL mouse recombinant IL-2 were added to the coculture. The proliferation of $CD8^+$ and $CD4^+$ T cells was measured by flow cytometer analysis after 3 days of coculture.

2.13. Measurements of L-Trp and Kyn in plasma

The kynurenine to tryptophan ratios in plasma in 4T1 tumor-bearing mice following different treatments were examined by HPLC as an indication of IDO enzyme activity. BALB/c mice bearing 4T1 tumors of ~200 mm^3 were treated with 5% glucose injection (as control), oxaliplatin (5 mg/kg), NLG919 (3.43 mg/kg), NLGplatin (8.63 mg/kg) or mixture of oxaliplatin and NLG919 (5 mg/kg oxaliplatin and 3.43 mg/kg NLG919) via i.p. administration every 3 days for 6 times. One day after the last treatment, the plasma samples were harvested about 100 μL. Then tubes were shaken for 1 min after 60 μL 6% perchloric acid added into the plasma samples and waited for 5 min. Subsequently, the tubes were centrifuged at 10,000 rpm for 10 min and the supernatants were used for test. A 20 μL of each solution was injected using SHIMADZU shim-pack C18 column and 90:10 water (containing 15 mM sodium acetate): acetonitrile buffer of pH 4.0 as mobile phase. The wavelength used for experiments were 360 nm for Kyn and 280 nm for Trp with the flow rate of 1 mL/min.

2.14. In vitro cytotoxicity of NLGplatin

The cytotoxic behaviors of oxaliplatin, NLGplatin and mixture of oxaliplatin and NLG919 were evaluated using MTT assay against 4T1 cells at 8 h. Cells were seeded on a 96-well plate at a density of 1×10^4 cells/well in 200 μL of desired medium and incubated for 24 h. The cells were treated with different compounds at varying concentrations and incubated for 8 h. Then, the cells were treated with 20 μL of MTT (5 mg/mL in Hanks) for 4 h. The medium was removed and the cells were lysed with 150 μL of DMSO, and absorbance of the purple formazan was recorded at 490 nm using Multiskan GO microplate reader. Each well was performed in five copies.

2.15. Cell cycle determination

4T1 cells were seeded at a density of 3×10^5 cells/mL on each well of a six well plate and allowed to grow overnight. 4T1 cancer cells treated with various drugs for 4 h before these drugs were treated with 1% FBS incomplete medium for 8 h. After 12 h treatment, cancer cells were washed in hanks and resuspended in hanks. Cells were then fixed in 70% ethanol overnight at −20 °C. Cells were then rehydrated with 1 mL of hanks, spun out of ethanol and then washed in hanks. Next, working solution (containing RNase A and PI) was used to resuspend the pellet. Cell cycle profiles were analyzed using NovoExpress 1.2.5.

2.16. Plasma pharmacokinetics

5 female BALB/c mice were i.p. administered with oxaliplatin and NLGplatin at a dose of 12 μM Pt per kg. Blood samples of 60 μL were withdrawn from the retro-orbital plexus/sinus of the mice from 0 min to 48 h (0 min, 5 min, 10 min, 30 min, 1 h, 2 h, 4 h, 6 h, 8 h, 12 h, 24 h and 48 h). The blood collected in heparinized tubes was centrifuged at 3500 rpm for 15 min. Supernatants were collected and determined by ICP-MS. The pharmacokinetic parameters were calculated based on a two-compartment model by DAS 2.0.

2.17. Statistics

All data are presented as mean ± Standard Error of Mean (s.e.m). Differences between groups were assessed using ANOVA and $P < 0.05$ was considered statistically significant.

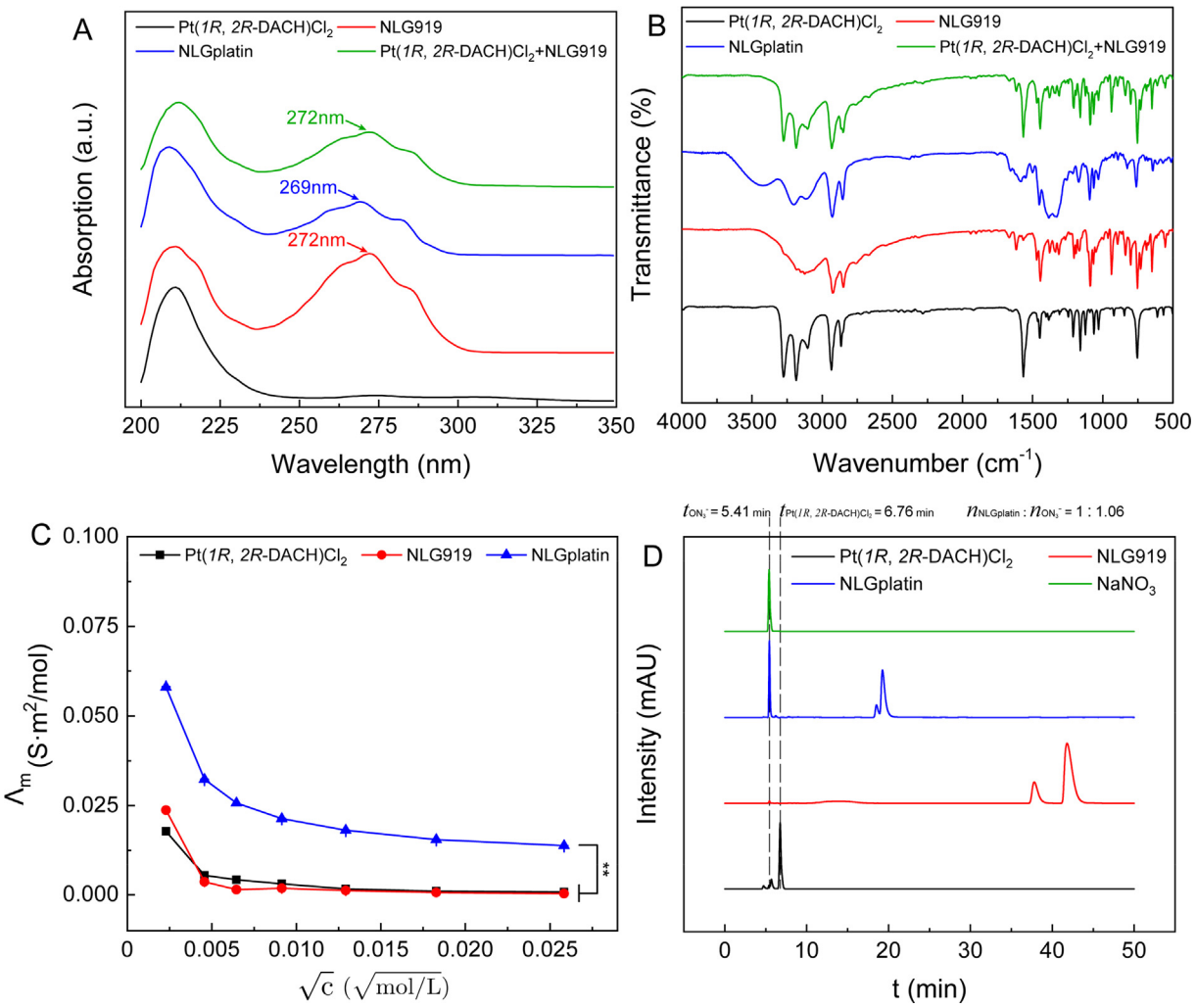

Fig. 1. Characterization of physicochemical properties of NLGplatin. (A) The UV spectra of Pt(*1R, 2R*-DACH)Cl_2, NLG919, NLGplatin or Pt(*1R, 2R*-DACH)Cl_2 mixing with NLG919 in methanol. (B) The IR spectra of Pt(*1R, 2R*-DACH)Cl_2, NLG919, NLGplatin or Pt(*1R, 2R*-DACH)Cl_2 mixing with NLG919. (C) The determination of conductivity with Pt(*1R, 2R*-DACH)Cl_2, NLG919 or NLGplatin in ultra-pure water. (D) The identification of nitrate ion by HPLC-UV at 215 nm with Pt(*1R, 2R*-DACH)Cl_2, NLG919, NLGplatin and $NaNO_3$.

3. Results and discussion

3.1. Characteristics of NLGplatin

NLGplatin was synthesized by silver nitrate precipitation method (Park et al., 2012) with Pt(*1R, 2R*-DACH)Cl_2 and NLG919 (Fig. S1). In order to identify the composition of NLGplatin, a variety of analytical methods were used to characterize it including electrospray ionization (ESI)-MS (Fig. S2), high resolution mass spectrometry (HRMS) (Fig. S3), ^1H and ^{13}C NMR spectroscopy (Fig. S4 and Fig. S5), and UV–vis spectra and infrared spectroscopic (IR) spectra (Fig. 1A and B). We found that the infrared spectrum of Pt(*1R, 2R*-DACH)Cl_2 physically mixing with NLG919 is very similar to that of Pt(*1R, 2R*-DACH)Cl_2 (Fig. 1B), but the compound, NLGplatin, showed a completely different spectrum as shown in Fig. 1B. In the 1000–1500 cm^{-1} and 2500–4000 cm^{-1}, there is infrared vibration absorption completely different from the physical mixing group, which means that NLGplatin was successfully synthesized.

And that NLGplatin can be dissolved in water (~2.23 mg/ml). This can be due to NLGplatin forming a salt with the nitrate ion in water. We detected conductivity with a series of concentration of three compounds in water by conductivity measurement experiment (Fig. 1C). NLGplatin showed us a significant difference among them that NLGplatin could be ionized in water into nitrate ion and platinum ion which was helpful for dissolve. We also used reversed phase high-performance liquid chromatography (RP-HPLC) to identify the presence of nitrate ion in NLGplatin (Fig. 1D). Nitrate ion and NLGplatin has a significant UV absorption at 215 nm (Fig. 1A). After HPLC identification, the compound of NLGplatin and the bulk drugs Pt(*1R, 2R*-DACH)Cl_2, NLG919 and nitrate ion can be completely separated, and the molar ratio of nitrate ion to NLGplatin is about 1:1. This result further confirmed the presence of nitrate ion in the structure of the NLGplatin.

3.2. Cellular uptake

We investigated the drug content of OXA and NLGplatin in 4T1 cells by cell uptake experiment as shown in Fig. 2A. NLGplatin appeared rapid accumulation after 1 h uptake contrary to OXA. Also, the concentration of NLGplatin in the nucleus was significantly higher than OXA. The reason why there is such difference between OXA and NLGplatin is due to the NLG919 in NLGplatin. The oil-water partition coefficient of NLG919 is 1.5, making it easy to penetrate the cell membrane (Li et al., 2014). Therefore, rapid and efficient uptake on NLGplatin may depend on the lipid permeation ability of NLG919 compared with OXA.

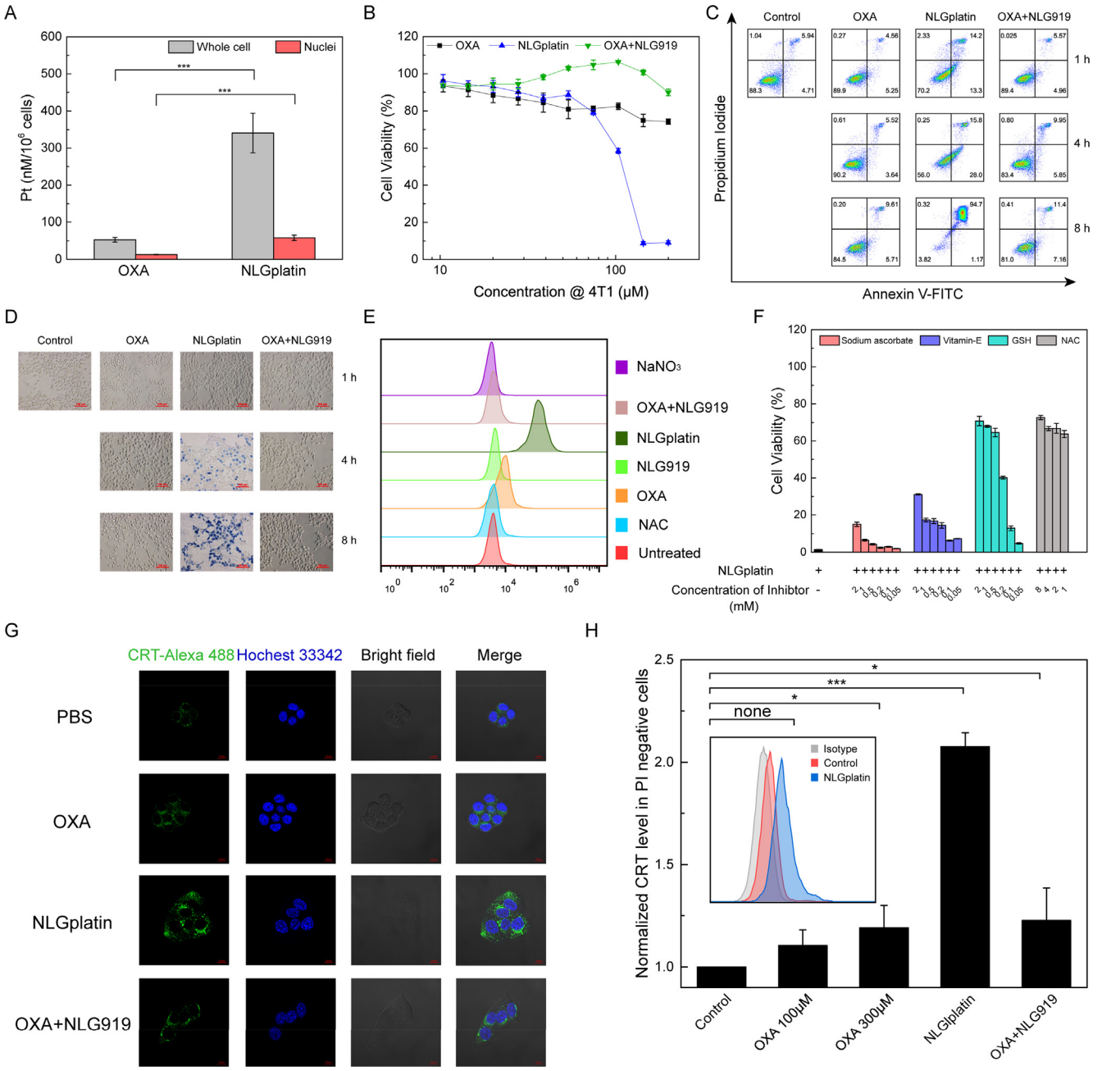

Fig. 2. In vitro biological characterizations of NLGplatin. (A) Intracellular uptake of Pt in 4T1 cells treated with OXA and NLGplatin. Cells were treated with 20 μM NLGplatin or OXA for 1 h. Platinum uptake was presented in units of Pt per nmol per liter of Pt per 10^6 cells. (B) Cytotoxicity of OXA, NLGplatin or OXA mixing with NLG919. Cells were treated for 8 h and cytotoxicity was determined by MTT assay. (C) Cytotoxicity of Pt agents in an Annexin V-FITC apoptosis assay. 4T1 cells were treated with different times and stained with Annexin V-FITC and propidium iodide. (D) Trypan blue rejection test by Pt agents at different times. (E) Determination of ROS *in vitro* by DCFH-DA assay. Cells were treated with different agents for 4 h and stained with DCFH-DA before fluorescence-activity cell sorting (FACS) analysis. (F) Cytotoxicity of NLGplatin and treated with different antioxidants for 8 h determined by MTT assay. (G) CRT exposure observed by confocal microscopy after drug treatment (4 h) of 4T1 cancer cells followed by stained with anti-CRT mAb. Scale bar is 10 μm. (H) 4T1 cancer cells were treated for 4 h (gated against PI negative cells) and surface-stained with anti-CRT pAb. Data represent means ± s.e.m. (G) and (H) were both using the Alexa Fluor® 488 antibody as secondary antibody. (For interpretation of the references to colour in this figure legend, the reader is referred to the web version of this article.)

3.3. In vitro cytotoxicity and cellular apoptosis

MTT assay result showed that NLGplatin had a better cytotoxic effect than OXA and showed obvious killing effect on tumor cells (Fig. 2B). Correspondingly, double staining of Annexin V-FITC and PI was carried out to investigate the apoptosis of cells under different time. As shown in Fig. 2C, NLGplatin caused large-scale apoptosis or necrosis in tumor cells at 8 h, and the trypan blue rejection assay further confirmed this result (Fig. 2D).

3.4. Intracellular ROS assay and CRT expression

Cell apoptosis could be due to a rapid accumulation of reactive oxygen species (ROS) induced by NLGplatin in cells. Then, DCFH-DA (a ROS probe) was used to measure intracellular ROS levels. As expected, NLGplatin can dramatically increase intracellular ROS levels in a short period of time (Fig. 2E), and only *N*-acetylcysteine (NAC) and glutathione (GSH) can prevent it effectively, while vitamin E could alleviate the damage (Fig. S6). Subsequently, when antioxidants such as

sodium ascorbate and vitamin E added with NLGplatin, cell viability could be partially reversed, whereas NAC and GSH can effectively control the increase of ROS and inhibit the killing of tumor cells by high concentration of NLGplatin (Fig. 2F). OXA has a weak effect on increasing ROS, and it cannot produce enough ROS to kill tumor cells in a short time, while NLGplatin can rapidly increase intracellular ROS levels in order to achieve the purpose of inducing tumor cell death (Wong et al., 2015; Ling et al., 2018). Consequently, the short-term cytotoxicity of NLGplatin is mainly due to its ability to produce enough ROS. A large amount of ROS will definitely affect the proliferation of cells and the cell cycle will change accordingly (Boonstra and Post, 2004). We found that changes in cell cycle of NLGplatin caused cells to be arrest in the G0/G1 phase because NLGplatin raised ROS to damage intracellular proteins (Fig. S7). Then, NLGplatin modified on the unit of OXA was able to increase ROS different from OXA itself, therefore, it is important to test if NLGplatin retains the ability of OXA to promote immunization and induces CRT exposure. NLGplatin treatment significantly increased the exposure of CRT (Fig. 2G) in immunofluorescence and expression level of CRT was determined by flow cytometer analysis (Fig. 2H) (Duan et al., 2016; He et al., 2016). This result indicates that NLGplatin retains the ability of OXA to promote CRT exposure in cell biology and own an extra function to significantly increase ROS levels.

3.5. Dissociation of NLGplatin

In order to confirm whether NLGplatin will degrade into OXA and NLG919 in the cellular environment, by measuring the intracellular drug contents, we found NLG919 has a significant concentration change in the cells over time (Fig. S8A and B) (Cheng et al., 2014). However, the compound NLGplatin did not have the form of NLG919 dissociation in cells. This also showed that NLGplatin did not release the NLG919 prototype drug in cells, but the whole effect of NLGplatin.

3.6. In vitro IDO assays and T-cell proliferation study

NLGplatin acquired ability to inhibit the IDO enzyme because NLG919 could block IDO enzyme which degraded L-Trp into Kyn (Fig. 3A) (Takikawa et al., 1988). The IC_{50} of NLG919 and NLGplatin on IFN-γ-induced HeLa cells were less than 10 μM while the IC_{50} of 1-methyl-tryptophan (1-MT) was up to 500 μM. Although the IC_{50} of NLGplatin was lower than NLG919, it was much better than 1-MT mainly because coordination of NLG919 in indoleamine ring did not influence the function of NLG919 (Liu et al., 2010; Peng et al., 2016). Similarly, OXA even at a very low concentration had a strong immunosuppressive effect on $CD4^+$ and $CD8^+$ T lymphocyte proliferation. However, proliferation inhibition was alleviated by mixture of OXA and NLG919 which meant NLG919 reduced immunosuppressive caused by OXA (Fig. 3B and C). Consequently, NLGplatin contained with NLG919 showed a significantly different phenomenon from OXA which meant that NLGplatin almost had no effect on lymphocyte proliferation. Due to the fact that OXA inhibited cellular protein synthesis of ribosomes, lymphocytes had no chance to synthesize enough proteins, whereas NLGplatin did not affect the function of ribosomes (Bruno et al., 2017).

3.7. Pharmacokinetics

After assessment of NLGplatin *in vitro*, we intended to study the pharmacokinetics of OXA and NLGplatin by intraperitoneal (i.p.) injection. Through pharmacokinetic analysis (Table 1), area under the concentration time curve (AUC) of NLGplatin was much more than OXA and peak concentration (Cmax) of NLGplatin was also significantly higher than OXA as well as a lower blood clearance (CL), which meant that NLGplatin circulated in the blood for longer than OXA and at a higher concentration (Fig. 4A). The significantly difference between NLGplatin and OXA mainly because the NLG919 part in NLGplatin is lipophilic which could help NLGplatin passes through the peritoneum but none of the same part in OXA.

In order to verify immunosuppression after chemotherapy, we measured the concentration of L-Trp and Kyn in blood (Zhao et al., 2011). And the results indicated that the systemic immunosuppressive effect of OXA group was significantly stronger than that of other groups (Fig. 4B). Interestingly, when mice treated with OXA combined with NLG919, immunosuppression level was consistent with control group no more than OXA, indicating that NLG919 relieved immunosuppression caused by OXA. Generally, chemotherapy drugs often bring about strong immune escape in the process of treating tumors. Clinical trials have also pointed out there are different levels of expression of IDO1 enzyme in a variety of tumor cells, whereas overexpression of IDO1 is unfavorable for the prognosis of patients (Uyttenhove et al., 2003). Therefore, we design a compound NLGplatin which can improve chemotherapy and enhance immunotherapy.

It is worth noting that the strategy we are proposed is based on the ability of platinum drugs and strong electron-donating compound to coordinate with each other. The advantage of this strategy is that it can connect two independent drugs into one item and exert different antitumor effects which are more advantageous than simple monotherapy. Unfortunately, since platinum compounds that have a permanent positive charge after coordination exhibit extremely high systemic toxicity *in vivo*, the maximum tolerated dose has been limited (Park et al., 2012; Johnstone et al., 2016; Hope et al., 2013). Encapsulated with liposomes or other negative charge materials maybe solve this problem in the future work.

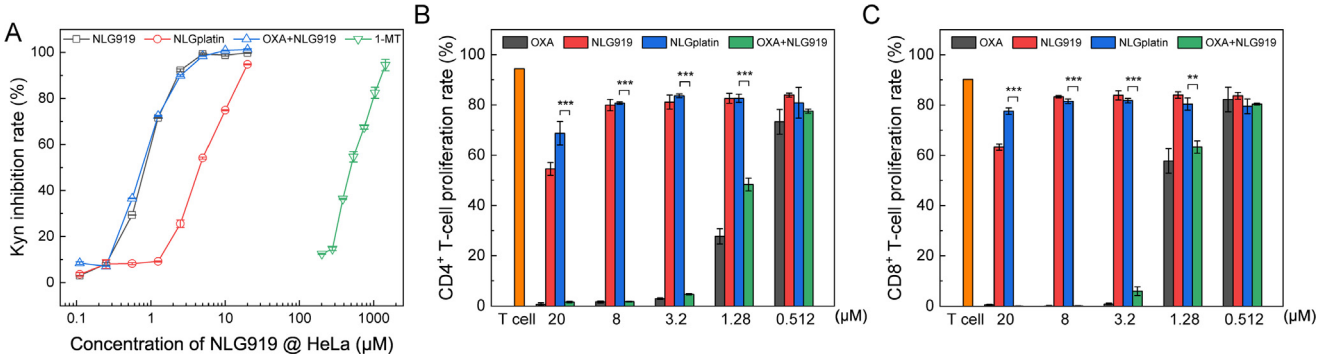

Fig. 3. The immunological properties of NLGplatin. (A) NLGplatin inhibited IDO enzyme activity *in vitro*. HeLa cells were treated with IFN-γ together with free NLG919, NLGplatin, mixture of OXA and NLG919 or 1-MT. Kynurenine in supernatants was measured 2 days later. Data represent means ± s.e.m. (B) $CD4^+$ and (C) $CD8^+$ T lymphocyte proliferation was examined by flow cytometer analysis. Data were means ± s.e.m. of 3 experiments. **P < 0.01 and ***P < 0.001.

Table 1
Pharmacokinetic parameters of OXA and NLGplatin.

Groups	$T_{1/2\alpha}$ (h)	$T_{1/2\beta}$ (h)	$AUC_{0\text{-}t}$ (μM × h)	C_{max} (μM)	CL (L/h/kg)	Vd (L/kg)	$MRT_{0\text{-}t}$ (h)
OXA	0.19 ± 0.05	32.07 ± 3.35	24.46 ± 1.72	3.81 ± 0.73	0.34 ± 0.04	2.53 ± 0.71	18.46 ± 0.64
NLGplatin	21.37 ± 15.47	47.90 ± 16.98	110.01 ± 9.17	5.27 ± 0.27	0.07 ± 0.01	3.13 ± 0.44	19.14 ± 1.19

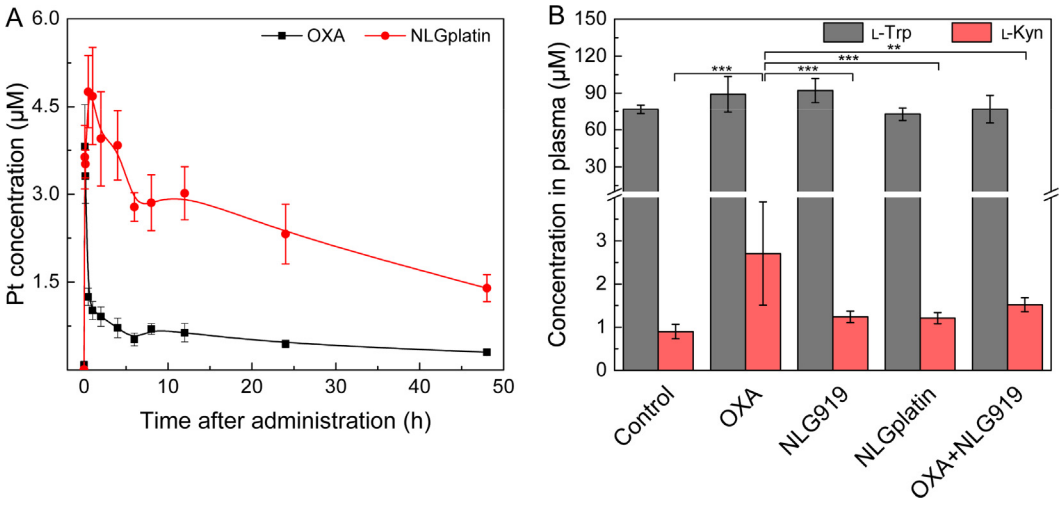

Fig. 4. (A) Blood kinetics of OXA and NLGplatin in BALB/c mice following i.p. administration of OXA or NLGplatin at a dose of 12 μM/kg. (B) The determination of L-Trp and Kyn in plasma. BALB/c mice bearing s.c. 4T1 tumors of ~200 mm^3 received 5% glucose injection (as a control), OXA, NLG919, NLGplatin or mixture of OXA and NLG919 i.p. once every 3 days for 6 times at dose of 12 μM/kg. Kynurenine and tryptophan in plasma were determined by RP-HPLC one day following last injection. Data were means ± s.e.m. of 5 experiments.

4. Conclusions

NLGplatin can kill tumor cells effectively without affecting the proliferation of immune cells. And NLGplatin is a new therapeutic agent composed of chemotherapy and immunotherapy. It retains the ability of inducing the exposure of CRT by unit of OXA and inhibiting the function of IDO1 enzyme with unit of NLG919 without affecting the lymphocyte proliferation which is distinct to OXA. It will become a potential drug for cancer treatment.

Declaration of Competing Interest

The authors declare that they have no known competing financial interests or personal relationships that could have appeared to influence the work reported in this paper.

Acknowledgments

This work was financially supported by the National Science and Technology Major Project (2017YFA0205400) and the National Natural Science Foundation of China (81773667, 81573369), and NSFC Projects of International Cooperation and Exchanges (81811540416). This work was also supported by the Fundamental Research Funds for the Central Universities (2632018PT01 and 2632018ZD12) and First-class Project (CPU2018GY06) and the "111" Project from the Ministry of Education of China and the State Administration of Foreign Experts Affairs of China (B16046). We thank the Cellular and Molecular Biology Center of China Pharmaceutical University for assistance with confocal microscopy work.

Appendix A. Supplementary material

Supplementary data to this article can be found online at https://doi.org/10.1016/j.ijpharm.2019.118736.

References

Boonstra, J., Post, J.A., 2004. Molecular events associated with reactive oxygen species and cell cycle progression in mammalian cells. Gene 337, 1–13.
Bruno, P.M., Liu, Y., Park, G.Y., Murai, J., Koch, C.E., Eisen, T.J., Pritchard, J.R., Pommier, Y., Lippard, S.J., Hemann, M.T., 2017. A subset of platinum-containing chemotherapeutic agents kills cells by inducing ribosome biogenesis stress. Nat. Med. 23, 461–471.
Chen, Y., Xia, R., Huang, Y., Zhao, W., Li, J., Zhang, X., Wang, P., Venkataramanan, R., Fan, J., Xie, W., Ma, X., Lu, B., Li, S., 2016. An immunostimulatory dual-functional nanocarrier that improves cancer immunochemotherapy. Nat. Commun. 7, 13443.
Cheng, Q., Shi, H., Wang, H., Min, Y., Wang, J., Liu, Y., 2014. The ligation of aspirin to cisplatin demonstrates significant synergistic effects on tumor cells. Chem. Comm. 50, 7427–7430.
Cheng, W., Nie, J., Gao, N., Liu, G., Tao, W., Xiao, X., Jiang, L., Liu, Z., Zeng, X., Mei, L., 2017. Cancer therapy: a multifunctional nanoplatform against multidrug resistant cancer: merging the best of targeted chemo/gene/photothermal therapy. Adv. Funct. Mater. 27, 1704135.
Duan, X., Chan, C., Guo, N., Han, W., Weichselbaum, R.R., Lin, W., 2016. Photodynamic therapy mediated by nontoxic core–shell nanoparticles synergizes with immune checkpoint blockade to elicit antitumor immunity and antimetastatic effect on breast cancer. J. Am. Chem. Soc. 138, 16686–16695.
Fan, Y.T., Zhou, T.J., Cui, P.F., He, Y.J., Chang, X., Xing, L., Jiang, H.L., 2019. Modulation of intracellular oxygen pressure by dual-drug nanoparticles to enhance photodynamic therapy. Adv. Funct. Mater. 29, 1806708.
Gabano, E., Ravera, M., Osella, D., 2014. Pros and cons of bifunctional platinum(IV) antitumor prodrugs: two are (not always) better than one. Dalton Trans. 43, 9813–9820.
Galluzzi, L., Senovilla, L., Zitvogel, L., Kroemer, G., 2012. The secret ally: immunostimulation by anticancer drugs. Nat. Rev. Drug Discov. 11, 215–233.
Green, D.R., Ferguson, T., Zitvogel, L., Kroemer, G., 2009. Immunogenic and tolerogenic cell death. Nat. Rev. Immunol. 9, 353–363.
He, C., Duan, X., Guo, N., Chan, C., Poon, C., Weichselbaum, R.R., Lin, W., 2016. Core-shell nanoscale coordination polymers combine chemotherapy and photodynamic therapy to potentiate checkpoint blockade cancer immunotherapy. Nat. Commun. 7, 12499.
Hope, J.M., Wilson, J.J., Lippard, S.J., 2013. Photoluminescent DNA binding and cytotoxic activity of a platinum(II) complex bearing a tetradentate beta-diketiminate ligand. Dalton Trans. 42, 3176–3180.
Johnstone, T.C., Suntharalingam, K., Lippard, S.J., 2016. The next generation of platinum drugs: targeted Pt(II) agents, nanoparticle delivery, and Pt(IV) prodrugs. Chem. Rev. 116, 3436–3486.
Lake, R.A., Robinson, B.W., 2005. Immunotherapy and chemotherapy-a practical partnership. Nat. Rev. Cancer 5, 397–405.
Li, M., Bolduc, A.R., Hoda, M.N., Gamble, D.N., Dolisca, S.B., Bolduc, A.K., Hoang, K.,

Ashley, C., McCall, D., Rojiani, A.M., Maria, B.L., Rixe, O., MacDonald, T.J., Heeger, P.S., Mellor, A.L., Munn, D.H., Johnson, T.S., 2014. The indoleamine 2,3-dioxygenase pathway controls complement-dependent enhancement of chemo-radiation therapy against murine glioblastoma. J. Immunother. Cancer 2, 21.

Liang, C., Wang, H., Zhang, M., Cheng, W., Li, Z., Nie, J., Liu, G., Lian, D., Xie, Z., Huang, L., Zeng, X., 2018. Self-controlled release of Oxaliplatin prodrug from d-α-tocopheryl polyethylene glycol 1000 succinate (TPGS) functionalized mesoporous silica nanoparticles for cancer therapy. J. Colloid Interface Sci. 525, 1–10.

Ling, X., Chen, X., Riddell, I.A., Tao, W., Wang, J., Hollett, G., Lippard, S.J., Farokhzad, O.C., Shi, J., Wu, J., 2018. Glutathione-scavenging poly(disulfide amide) nanoparticles for the effective delivery of Pt(IV) prodrugs and reversal of cisplatin resistance. Nano Lett. 18, 4618–4625.

Liu, X., Shin, N., Koblish, H.K., Yang, G., Wang, Q., Wang, K., Leffet, L., Hansbury, M.J., Thomas, B., Rupar, M., Waeltz, P., Bowman, K.J., Polam, P., Sparks, R.B., Yue, E.W., Li, Y., Wynn, R., Fridman, J.S., Burn, T.C., Combs, A.P., Newton, R.C., Scherle, P.A., 2010. Selective inhibition of IDO1 effectively regulates mediators of antitumor immunity. Blood 115, 3520–3530.

Lob, S., Konigsrainer, A., Rammensee, H.G., Opelz, G., Terness, P., 2009. Inhibitors of indoleamine-2,3-dioxygenase for cancer therapy: can we see the wood for the trees? Nat. Rev. Cancer 9, 445–452.

Lu, J., Liu, X., Liao, Y.P., Salazar, F., Sun, B., Jiang, W., Chang, C.H., Jiang, J., Wang, X., Wu, A.M., Meng, H., Nel, A.E., 2017. Nano-enabled pancreas cancer immunotherapy using immunogenic cell death and reversing immunosuppression. Nat. Commun. 8, 1811.

Muller, A.J., Prendergast, G.C., 2005. Marrying immunotherapy with chemotherapy: why say IDO? Cancer Res. 65, 8065–8068.

Obeid, M., Tesniere, A., Ghiringhelli, F., Fimia, G.M., Apetoh, L., Perfettini, J.L., Castedo, M., Mignot, G., Panaretakis, T., Casares, N., Metivier, D., Larochette, N., van Endert, P., Ciccosanti, F., Piacentini, M., Zitvogel, L., Kroemer, G., 2007. Calreticulin exposure dictates the immunogenicity of cancer cell death. Nat. Med. 13, 54–61.

Park, G.Y., Wilson, J.J., Song, Y., Lippard, S.J., 2012. Phenanthriplatin, a monofunctional DNA-binding platinum anticancer drug candidate with unusual potency and cellular activity profile. Proc. Natl. Acad. Sci. 109, 11987–11992.

Peng, Y.H., Ueng, S.H., Tseng, C.T., Hung, M.S., Song, J.S., Wu, J.S., Liao, F.Y., Fan, Y.S., Wu, M.H., Hsiao, W.C., Hsueh, C.C., Lin, S.Y., Cheng, C.Y., Tu, C.H., Lee, L.C., Cheng, M.F., Shia, K.S., Shih, C., Wu, S.Y., 2016. Important hydrogen bond networks in indoleamine 2,3-dioxygenase 1 (IDO1) inhibitor design revealed by crystal structures of imidazoleisoindole derivatives with IDO1. J. Med. Chem. 59, 282–293.

Qiao, J.B., Fan, Q.Q., Xing, L., Cui, P.F., He, Y.J., Zhu, J.C., Wang, L., Pang, T., Oh, Y.K., Zhang, C., Jiang, H.L., 2018. Vitamin a-decorated biocompatible micelles for chemogene therapy of liver fibrosis. J. Controlled Release 283, 113–125.

Shi, J., Kantoff, P.W., Wooster, R., Farokhzad, O.C., 2017. Cancer nanomedicine: progress, challenges and opportunities. Nat. Rev. Cancer 17, 20–37.

Takikawa, O., Kuroiwa, T., Yamazaki, F., Kido, R., Mechanism of interferon-gamma action, 1988. Characterization of indoleamine 2, 3-dioxygenase in cultured human cells induced by interferon-gamma and evaluation of the enzyme-mediated tryptophan degradation in its anticellular activity. J. Biol. Chem. 263, 2041–2048.

Uyttenhove, C., Pilotte, L., Theate, I., Stroobant, V., Colau, D., Parmentier, N., Boon, T., Van den Eynde, B.J., 2003. Evidence for a tumoral immune resistance mechanism based on tryptophan degradation by indoleamine 2,3-dioxygenase. Nat. Med. 9, 1269–1274.

Vanneman, M., Dranoff, G., 2012. Combining immunotherapy and targeted therapies in cancer treatment. Nat. Rev. Cancer 12, 237–251.

Wang, N., Wang, Z.G., Xu, Z.F., Chen, X.F., Zhu, G.Y., 2018. A cisplatin-loaded immunochemotherapeutic nanohybrid bearing immune checkpoint inhibitors for enhanced cervical cancer therapy. Angew. Chem. Int. Ed. 57, 3426–3430.

Wong, D.Y., Ong, W.W., Ang, W.H., 2015. Induction of immunogenic cell death by chemotherapeutic platinum complexes. Angew. Chem. Int. Ed. 54, 6483–6487.

Xing, L., Zhang, J.L., Zhou, T.J., He, Y.J., Cui, P.F., Gong, J.H., Sun, M., Lu, J.J., Huang, Z., Jin, L., Jiang, H.L., 2018. A novel design of a polynuclear co-delivery system for safe and efficient cancer therapy. Chem. Comm. 54, 8737–8740.

Zeng, X., Luo, M., Liu, G., Wang, X., Tao, W., Lin, Y., Ji, X., Nie, L., Mei, L., 2018. Polydopamine-modified black phosphorous nanocapsule with enhanced stability and photothermal performance for tumor multimodal treatments. Adv. Sci. 5, 1800510.

Zhao, J., Chen, H., Ni, P., Xu, B., Luo, X., Zhan, Y., Gao, P., Zhu, D., 2011. Simultaneous determination of urinary tryptophan, tryptophan-related metabolites and creatinine by high performance liquid chromatography with ultraviolet and fluorimetric detection. J. Chromatogr. B 879, 2720–2725.